

# Synthesis and sinterability of composite powder of the TiB<sub>2</sub>–B<sub>4</sub>C system

Hideaki Itoh, Yuji Tsunekawa, Shin-ichi Tago and Hiroyasu Iwahara

Synthetic Crystal Research Laboratory, School of Engineering, Nagoya University, Furo-cho, Chikusa-ku, Nagoya 464-01 (Japan)

(Received July 14, 1992)

## Abstract

Composite powders of composition TiB<sub>2</sub>–x B<sub>4</sub>C (x = 0.3, 0.5, 0.7 and 1.0) were synthesized by a solid state reaction between TiC<sub>x</sub>N<sub>1–x</sub> and amorphous boron. The formation of TiB<sub>2</sub> and B<sub>4</sub>C occurs by a stepwise process: (1) the formation of TiB<sub>2</sub> by the substitution of boron for carbon or nitrogen atoms in TiC<sub>x</sub>N<sub>1–x</sub>; (2) the simultaneous or subsequent formation of B<sub>4</sub>C by the reaction between unreacted boron and free carbon released from TiC<sub>x</sub>N<sub>1–x</sub>. The formation reaction of a well-dispersed composite powder of the TiB<sub>2</sub>–x B<sub>4</sub>C system was completed by heat treatment of the starting powder mixed in the mole ratio TiC<sub>x</sub>N<sub>1–x</sub>: B = 1:(4x + 2) under a flowing argon atmosphere at 1500 °C for 60 min. The synthesized powder, which was densified at 4 GPa and 1600 °C for 15 min, exhibited favourable sinterability. The sintered compact showed a relative density of 93.7%–97.0% and a Vickers microhardness of 35.3–37.3 GPa depending on the composition.

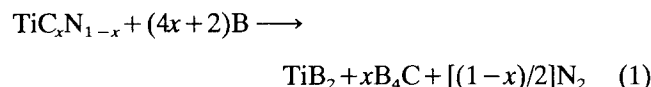
## 1. Introduction

Titanium diboride (TiB<sub>2</sub>) and boron carbide (B<sub>4</sub>C) have high melting points and hardnesses as well as low densities compared with those of other transition metal borides and carbides [1] as seen in Table 1. The thermal expansion coefficients of the two compounds are quite similar, but the electrical conductivity varies from metallic (TiB<sub>2</sub>) to semiconducting (B<sub>4</sub>C) behaviour. However, TiB<sub>2</sub> and B<sub>4</sub>C are difficult to sinter [2] and several composite systems based on the two boron compounds have been investigated in order to prepare dense sintered compacts [3–10].

Sintered composites based on the TiB<sub>2</sub>–B<sub>4</sub>C system are expected to be useful for corrosion- and wear-resistant tools or electrode materials if a successful processing route can be developed. A fine-grained composite powder with a homogeneous distribution of TiB<sub>2</sub> and B<sub>4</sub>C is required to prepare dense and tough sintered compacts in this system [11].

Recent papers describe a new procedure to synthesize fine TiB<sub>2</sub> powder by a controlled solid state reaction

between titanium nitride (TiN) and amorphous boron [12, 13] and the subsequent preparation of sintered single-phase TiB<sub>2</sub> compacts by hot pressing [14]. A similar formation reaction for the synthesis of mixed TiB<sub>2</sub>–B<sub>4</sub>C powder would be the solid state reaction between titanium carbonitride (TiC<sub>x</sub>N<sub>1–x</sub>) powder and amorphous boron powder according to



In the present work the synthesis of TiB<sub>2</sub>–B<sub>4</sub>C composite powder was investigated by varying the value of x from 0.3 to 1.0. The sinterability of the synthesized powder was investigated by high pressure sintering.

## 2. Experimental details

### 2.1. Synthesis and sintering of composite powder

Commercially available TiC<sub>x</sub>N<sub>1–x</sub> powders (Nihon Sin-Kinzoku Co., grain size 1.3–1.4 μm, purity better

TABLE 1. Properties of TiB<sub>2</sub> and B<sub>4</sub>C

	Density (g/cm <sup>3</sup> )	Melting point (°C)	Hardness Hv (kg/mm <sup>2</sup> )	Resistivity (Ω cm)	Thermal expansion coefficient (deg <sup>-1</sup> )
TiB <sub>2</sub>	4.53	2790	3400	9 × 10 <sup>-6</sup>	4.6 × 10 <sup>-6</sup>
B <sub>4</sub> C	2.51	2450	4200	1	4.5 × 10 <sup>-6</sup>

than 96 wt.%) and amorphous boron (Rare Metallic Co., grain size 0.5–3  $\mu\text{m}$ , purity better than 96.6 wt.%) were used as starting materials. The compositions of the as-received  $TiC_xN_{1-x}$  powders ( $x=0.3, 0.5, 0.7$  and 1.0) were confirmed by X-ray measurements of the lattice constants. The initial powders were heat treated separately at 600 °C for 60 min in vacuum and subsequently mixed in an agate mortar in the mole ratio  $TiC_xN_{1-x}:B=1:(4x+2)$ , the net contents of  $TiC_xN_{1-x}$  and boron in the as-received powders being used for the calculation of the mole ratio. The mixed powder was again pretreated under vacuum ( $1 \times 10^{-5}$  Torr) at 600 °C for 60 min and subsequently heated in an argon stream (flow rate 60 ml  $\text{min}^{-1}$ ) for 40 min to a given temperature in the range between 900 and 1500 °C. The soaking time was varied between 0 and 360 min. Finally, the synthesized powder was densified at 4 GPa and 1600 °C for 15 min in a girdle-type high pressure apparatus [15].

## 2.2. Analysis and evaluation of synthesized powder and sintered compact

The synthesized powder and sintered compact were characterized by X-ray diffraction. The relative amount formed and the crystallinity of each crystalline phase were evaluated by the relative intensities of the specified diffraction lines, 101 for  $TiB_2$ , 021 for  $B_4C$  and 200 for  $TiC_xN_{1-x}$ , using the 220 line for silicon as an internal standard. Commercial well-crystallized powders of  $TiB_2$  and  $B_4C$  were used for comparison of the crystallinity of the synthesized powder. The contents of Ti and B in the synthesized powders were measured by inductively coupled plasma (ICP) emission analysis. The synthesized powders and the fractured or polished surfaces of the sintered compacts were examined by scanning electron microscopy (SEM) and X-ray microanalysis (XMA). The bulk density of the sintered compact was measured by Archimedes' method and the Vickers microhardness was measured with a load of 0.5 kgf.

## 3. Results and discussion

### 3.1. Effects of treatment temperature on the formation of $TiB_2$ - $B_4C$ powder

The influence of treatment temperature on the formation of  $TiB_2$  and  $B_4C$  was examined in the temperature range 900–1500 °C with a constant holding time of 60 min. Figure 1 shows the relation between relative X-ray intensity ( $I/I_{Si}$ ) of each phase and treatment temperature for  $x=1$ , i.e. starting powder composition  $TiC+6B$ . The X-ray diffraction patterns of the products obtained at 1000, 1200 and 1500 °C are shown in Fig. 2. A small amount of  $TiB_2$  is already detectable at 900 °C and this amount increases progressively with

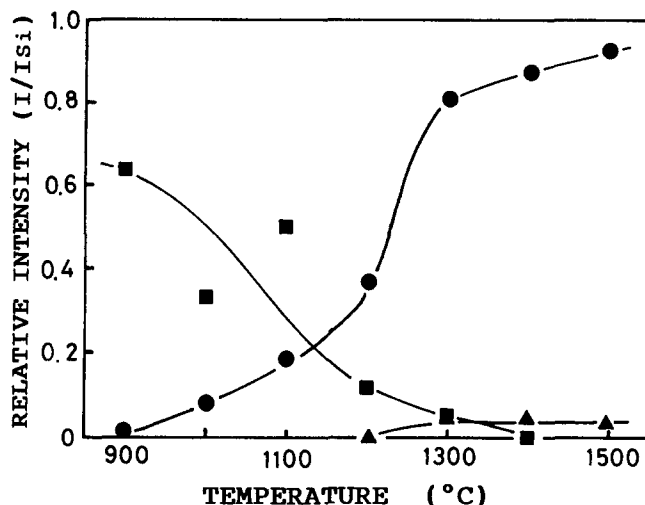


Fig. 1. Relative X-ray intensity plotted against treatment temperature; holding time 60 min; starting powder composition  $TiC+6B$ ; ●,  $TiB_2$ ; ▲,  $B_4C$ ; ■,  $TiC$ .

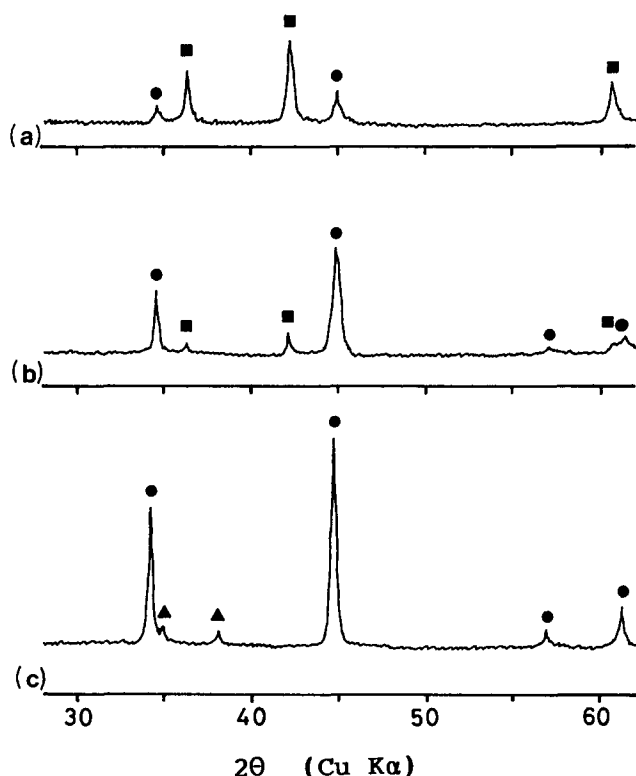


Fig. 2. X-ray diffraction patterns of specimens heat treated at (a) 1000, (b) 1200 and (c) 1500 °C for 60 min; starting powder composition  $TiC+6B$ ; ●,  $TiB_2$ ; ▲,  $B_4C$ ; ■,  $TiC$ .

increasing temperature up to 1200 °C, while the amount of  $TiC$  decreases (see Figs. 2(a) and 2(b)). Amorphous boron cannot be detected by X-ray diffraction. The following substitution reaction would proceed in the low temperature range, resulting in the formation of crystalline  $TiB_2$  and amorphous carbon:



A trace of  $B_4C$  was detected at 1300 °C, as shown in Fig. 1. In the temperature range 1200–1300 °C a steep increase in the relative intensity of  $TiB_2$  was observed owing to the accelerated formation reaction of  $TiB_2$ . The crystallinity of  $TiB_2$  was found to be comparable with that of commercial well-crystallized  $TiB_2$ . In the intermediate temperature range the solid state reaction between unreacted boron and free carbon would take place in addition to reaction (2):



The following direct formation reaction of  $TiB_2$  and  $B_4C$  between  $TiC$  and amorphous boron would also proceed simultaneously with the stepwise reactions (2) and (3):



Above 1300 °C a gradual increase in the relative intensity of  $TiB_2$  is observed. However, the relative intensity of  $B_4C$  did not increase even at this elevated temperature (see Fig. 2(c)), where the crystallinity was estimated to be low compared with that of commercial well-crystallized  $B_4C$ .

Figure 3 shows the relation between relative X-ray intensity and treatment temperature for  $x=0.3$ , i.e. the starting powder composition  $TiC_{0.3}N_{0.7} + 3.2B$ . Analogous formation of  $TiB_2$  and  $B_4C$  was observed, except that a steep increase in the relative intensity was not seen in the temperature range 1200–1300 °C. According to reaction (1), nitrogen gas would be generated and removed from the reaction system [12]. For both  $x=0.5$  and 0.7 a similar temperature dependence of the relative intensity as shown in Fig. 3 was observed, although the formation of  $TiB_2$  was slightly depressed with decreasing

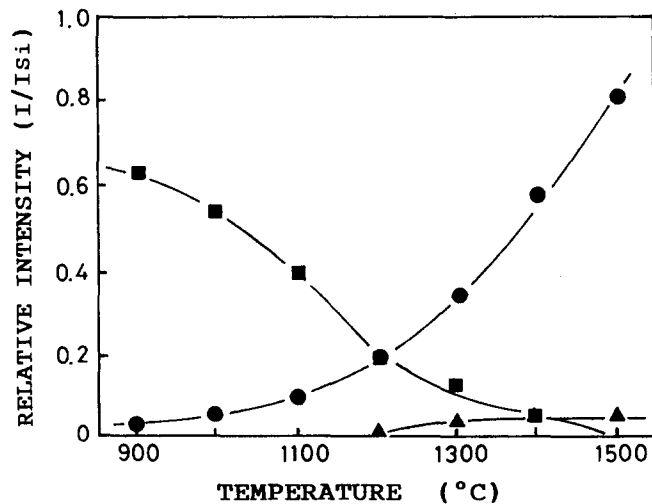


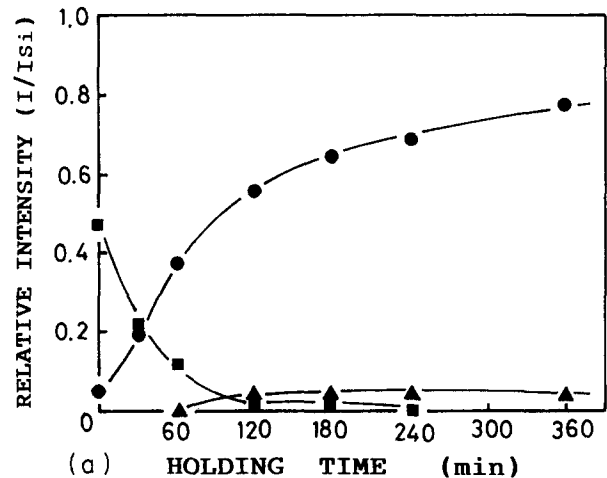
Fig. 3. Relative X-ray intensity plotted against treatment temperature; holding time 60 min; starting powder composition  $TiC_{0.3}N_{0.7} + 3.2B$  ( $x=0.3$ ); ●,  $TiB_2$ ; ▲,  $B_4C$ ; ■,  $TiC_{0.3}N_{0.7}$ .

value of  $x$ . This could be attributed to the different stabilities of each  $TiC_xN_{1-x}$  composition.

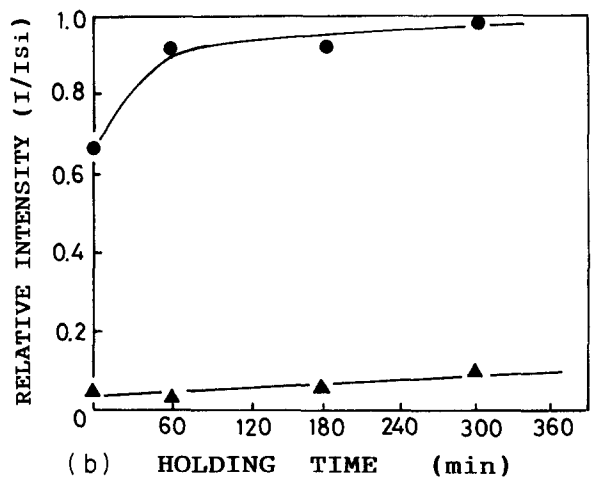
### 3.2. Effects of holding time on the formation of $TiB_2-B_4C$ powder

Figures 4(a) and 4(b) show the relation between relative X-ray intensity and holding time for a starting powder composition  $x=1$  and treatment temperatures of 1200 and 1500 °C respectively.  $TiB_2$  formed at 1200 °C according to reaction (2) up to 60 min, after which  $B_4C$  began to form, but  $TiC$  remained in coexistence up to 240 min. A holding time of over 240 min was required in order to complete the formation reaction of the composite powder comprising crystalline  $TiB_2$  and low crystalline  $B_4C$ . However, at 1500 °C it is found in Fig. 4(b) that the  $TiB_2-B_4C$  composite powder can be synthesized even without soaking by the direct formation reaction of both powders according to reaction (4).

Figure 5 shows the relationship between relative X-ray intensity and holding time for a starting powder



(a) HOLDING TIME (min)



(b) HOLDING TIME (min)

Fig. 4. Relative X-ray intensity as a function of holding time; treatment temperatures (a) 1200 and (b) 1500 °C; starting powder composition  $TiC + 6B$ ; ●,  $TiB_2$ ; ▲,  $B_4C$ ; ■,  $TiC$ .

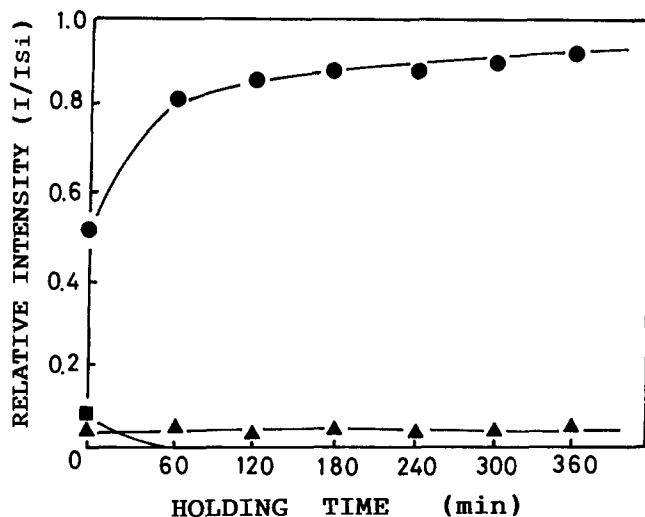


Fig. 5. Relative X-ray intensity as a function of holding time; treatment temperature 1500 °C; starting powder composition  $Ti_{0.3}N_{0.7} + 3.2B$  ( $x=0.3$ ); ●,  $TiB_2$ ; ▲,  $B_4C$ ; ■,  $TiC_{0.3}N_{0.7}$ .

composition  $x=0.3$  and a treatment temperature of 1500 °C. A composite powder of composition  $TiB_2-0.3B_4C$  was synthesized after a holding time of 60 min. At the treatment temperature of 1200 °C, however, the solid state reaction (4) did not complete even after 360 min, with a residual  $TiC_{0.3}N_{0.7}$  detected.

### 3.3. Surface appearance of synthesized composite powder

Figure 6 shows scanning electron micrographs of the surface appearance of the composite powders synthesized under the treatment conditions of 1500 °C for 60 min using the starting powder compositions  $x=0.3$ , 0.7 and 1.0. It was confirmed by ICP emission analysis that the atomic ratios Ti:B of the synthesized powders correspond to those of the starting powder compositions ( $1:(4x+2)$ ). In the specimen with  $x=0.3$  a homoge-

neously mixed powder of  $TiB_2$  and  $B_4C$  can be seen, where the white-coloured grains are  $TiB_2$  and the grey-coloured grains are  $B_4C$ . The grain size of  $TiB_2$  is 1.5–2.0  $\mu m$ , which is a little larger than that of the starting  $TiC_xN_{1-x}$  powder. This suggests that the formation of the composite powder would occur by the substitution of boron for carbon or nitrogen atoms and the crystallization of  $TiB_2$  within the  $TiC_xN_{1-x}$  particles. Neither coagulation nor partial sintering of the powder was observed. The formation of  $B_4C$  around the  $TiB_2$  particles would lead to the good dispersibility of the synthesized powder. The amount of  $B_4C$  is found to increase with increasing  $x$ , as seen by the fine-grained  $B_4C$  powder covering the  $TiB_2$  grains in Figs. 6(b) and 6(c). Some coagulation of the synthesized powder was observed, however, in the case of a longer treatment time of 360 min, with increasing crystallinity of the  $TiB_2$  grains.

### 3.4. Sinterability of synthesized composite powder

Table 2 shows the bulk density and microhardness of the sintered compacts which were prepared at 4 GPa and 1600 °C for 15 min from the synthesized composite powder of various compositions ( $x=0.3$ , 0.5, 0.7 and 1.0). The density increased as the  $x$  value decreased and a sintered compact with a relative density of 97.0% was obtained at  $x=0.3$  (i.e.  $TiB_2+0.3B_4C$ ). The density of the specimen with  $x=0.7$  increased from 93.7% to 95.6% with increasing heat treatment time from 60 to 300 min. The microhardness of the composite sintered compact is found to increase linearly with composition  $x$ , which verifies that the hardness depends on the composition ratio  $B_4C:TiB_2$ .

Figure 7 shows the X-ray diffraction pattern of the surface of a sintered compact of the  $TiB_2-0.3B_4C$  system. The existence of highly crystallized  $TiB_2$  and low crystalline  $B_4C$  was confirmed by comparison with the crystallinity of commercial  $TiB_2$  and  $B_4C$ . Figure 8

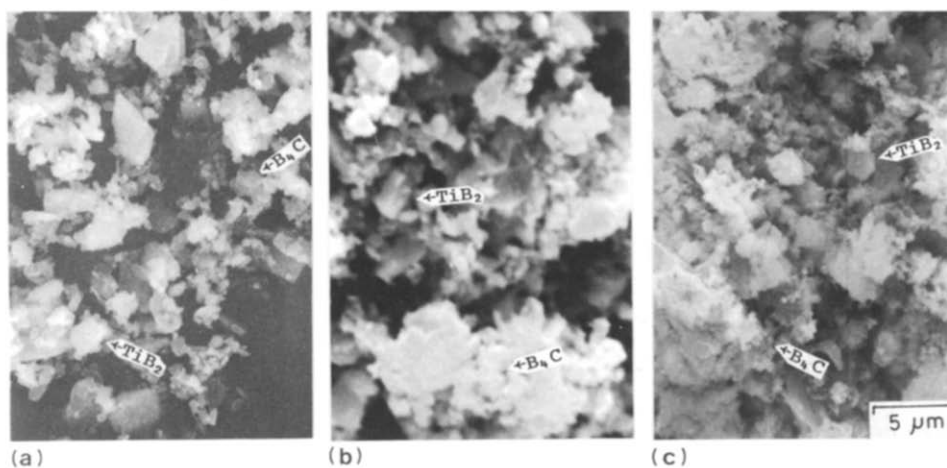


Fig. 6. Scanning electron micrographs of composite powder  $TiB_2 + xB_4C$ ; treatment temperature 1500 °C; holding time 60 min;  $x=(a)$  0.3, (b) 0.7 and (c) 1.0.

TABLE 2. Bulk density and microhardness of the composite sintered compact prepared at 4 GPa and 1600 °C for 15 min

Composition (x)	Bulk density (g/cm <sup>3</sup> )	Relative density (%)	Microhardness (kg/mm <sup>2</sup> )
0.3	3.78	97.0	3630
0.5	3.56	96.7	3680
0.7	3.31	93.7	3760
1.0	3.04	91.0	3860

Synthetic conditions of composite powder: 1500 °C, 60 min.

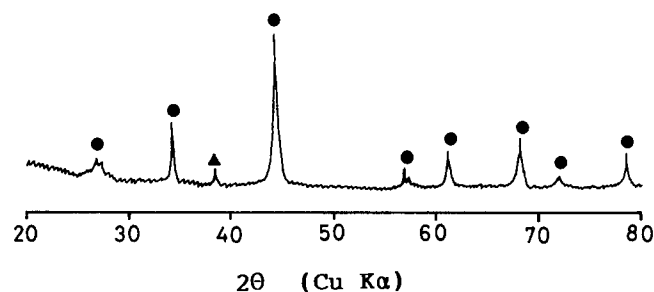


Fig. 7. X-ray diffraction pattern of surface of sintered compact of TiB<sub>2</sub>-0.3B<sub>4</sub>C; ●, TiB<sub>2</sub>; ▲, B<sub>4</sub>C.

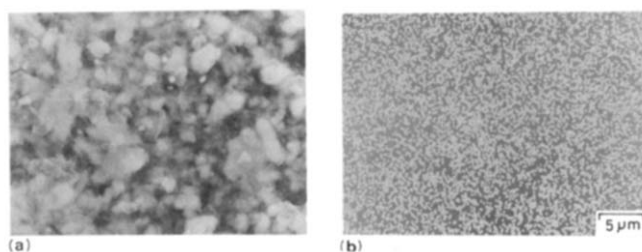


Fig. 8. XMA images of sintered compact of TiB<sub>2</sub>-0.3B<sub>4</sub>C; (a) reflected electron image; (b) Ti K $\alpha$  image.

shows (a) the electron reflection image of the polished surface of the same sintered compact and (b) the XMA image of Ti K $\alpha$ . The homogeneous distribution of TiB<sub>2</sub> and B<sub>4</sub>C grains is confirmed. Therefore the sintered composite is considered to be composed of fine-grained and well-crystallized TiB<sub>2</sub> grains dispersed in a low crystalline B<sub>4</sub>C matrix.

#### 4. Conclusions

Composite powders of the TiB<sub>2</sub>-B<sub>4</sub>C system were synthesized by a solid state reaction between TiC<sub>x</sub>N<sub>1-x</sub>

and amorphous boron and the sinterability of the synthesized powder was evaluated by high pressure sintering. The results can be summarized as follows.

(1) Fine-grained composite powders of composition TiB<sub>2</sub>+xB<sub>4</sub>C ( $x=0.3, 0.5, 0.7$  and  $1.0$ ) were synthesized by heat treatment of the TiC<sub>x</sub>N<sub>1-x</sub> and B starting powders mixed in the ratio of  $1:(4x+2)$  in an argon stream at 1500 °C for 60 min. The substitution of boron for carbon or nitrogen atoms and the simultaneous or subsequent reaction between unreacted boron and free carbon released from TiC<sub>x</sub>N<sub>1-x</sub> occur to form a well-dispersed TiB<sub>2</sub>-B<sub>4</sub>C composite powder.

(2) The synthesized powder was sintered at 4 GPa and 1600 °C for 15 min. The relative density of the sintered composite increased to 97.0% at  $x=0.3$ . The sintered compact was composed of fine-grained and well-crystallized TiB<sub>2</sub> grains dispersed in a low crystalline B<sub>4</sub>C matrix. The microhardness increased with increasing B<sub>4</sub>C content.

Details of the microstructure and the mechanical, electrical and oxidation resistance properties of the sintered composite will be reported in another paper.

#### References

- 1 G. V. Samsonov and I. M. Vinitkii, *Handbook of Refractory Compounds*, IFI/Plenum, New York, 1980, p. 1.
- 2 S. L. Dole, S. Prochazka and R. H. Doremus, *J. Am. Ceram. Soc.*, 72 (1989) 958.
- 3 T. Watanabe and S. Kouno, *Ceram. Bull.*, 61 (1982) 970.
- 4 D. C. Halverson, A. J. Pyzik, I. A. Aksay and W. E. Snowden, *J. Am. Ceram. Soc.*, 72 (1989) 775.
- 5 T. Watanabe, *Funtai-oyobi-Funmatsu-Yakin*, 36 (1989) 365.
- 6 J. D. Whittenberger, R. K. Viswanadham, S. K. Mannan and B. Sprissler, *J. Mater. Sci.*, 25 (1990) 35.
- 7 T. Tani and S. Wada, *J. Mater. Sci.*, 25 (1990) 157.
- 8 T. Tani and S. Wada, *J. Mater. Sci. Lett.*, 9 (1990) 22.
- 9 W. A. Zdaniewski, *Am. Ceram. Soc. Bull.*, 65 (1986) 1408.
- 10 C. H. MacMurthy, W. D. G. Boecker, S. G. Seshadri, J. S. Zanghi and J. E. Garnier, *Am. Ceram. Soc. Bull.*, 66 (1987) 325.
- 11 E. S. Kang, C. W. Jang, C. H. Lee and C. H. Kim, *J. Am. Ceram. Soc.*, 72 (1989) 1868.
- 12 T. Matsudaira, H. Itoh, S. Naka, H. Hamamoto and M. Obayashi, *J. Mater. Sci.*, 23 (1988) 288.
- 13 H. Itoh, T. Matsudaira, S. Naka and H. Hamamoto, *J. Mater. Sci.*, 24 (1989) 420.
- 14 H. Itoh, S. Naka, T. Matsudaira and H. Hamamoto, *J. Mater. Sci.*, 25 (1990) 533.
- 15 H. Itoh, S. Tajima, M. Tamaki and S. Naka, *J. Mater. Sci.*, 23 (1988) 2877.